doi: 10.4149/gpb_2026027

Transcription factor KLF4 suppresses the malignant progression of colorectal cancer by activating ETFDH transcription

Yan Zeng[1], Qiaozhen Liu[1], Yali Xu[1], Tong Zhao[1] and Zhiping Hu[1]

[1] *Department of Abdominal Tumors II, Jiujiang Third People's Hospital, Jiujiang, China*

Abstract. Colorectal cancer (CRC) is a common cause of cancer-related deaths worldwide. Electron transfer flavoprotein dehydrogenase (ETFDH) is a novel prognostic biomarker for human CRC. However, the role and molecular mechanism of ETFDH in CRC are still unclear. DEGs in CRC development were identified using mRNA microarray datasets GSE23011, GSE44076, and GSE113513. Gene expression was determined using RT-qPCR and Western blot. Cell proliferation, migration, and invasion were detected by EdU, Colony formation, Transwell, and wound healing. Effects of CRC cells on $CD8^+$ T cell apoptosis were analyzed using flow cytometry. Effects of ETFDH on CRC cell growth *in vivo* was analyzed using xenograft model. After JASPAR prediction, the binding between Transcription factor Kruppel-like factor 4 (KLF4) and ETFDH promoter was verified using ChIP and dual-luciferase reporter. ETFDH and KLF4 were decreased in CRC tissues and cells. ETFDH upregulation blocked CRC cell proliferation, migration, invasion, and repress the apoptosis of $CD8^+$ T cells *in vitro*. ETFDH overexpression hindered CRC tumor growth *in vivo.* Mechanistically, KLF4 enhanced the transcriptional activity of ETFDH *via* binding to its promoter region. KLF4-activated ETFDH transcription suppresses CRC cell malignant behavior and decreases the apoptosis of $CD8^+$T cells, which provides a promising therapeutic target for CRC.

Key words: Colorectal cancer — Electron transfer flavoprotein dehydrogenase gene — KLF4 — Proliferation — $CD8^+$ T cells — Apoptosis

Introduction

As a prevalent gastrointestinal malignancy, colorectal cancer (CRC) has become a major public health concern and brings a heavy economic and societal burden in many countries, particularly in China, with increasing incidence and mortality rates annually (Qu et al. 2022; Shin et al. 2023). Nevertheless, current understanding of its pathogenesis and treatment strategies remains limited. Although traditional treatment approaches, such as early diagnosis, screening, surgery, radiotherapy, chemotherapy, and targeted drugs, have made significant progress in clinical application, most CRC patients are identified at an advanced stage involving metastatic tumors with high resistance, leading to poor prognosis (Biller and Schrag 2021; Abedizadeh et al. 2024; Mou et al. 2025). Accordingly, exploring the potential mechanism of CRC is crucial for alternative therapeutic strategies.

Increasing evidence has indicated that immune checkpoint blockade presents durable responses and long-lasting clinical benefits for many types of solid tumors, inducing CRC (Ganesh et al. 2019; Weng et al. 2022). As an important immune checkpoint protein, programmed death ligand-1 (PD-L1), a 33 kDa type I transmembrane glycoprotein, is able to downregulate T-cell function and cell survival through binding to programmed death-1 (PD-1) receptor on T cell surface, which are the primary effector cells in antitumor immunity (Lee et al. 2024). Furthermore, it has been reported that PD-L1 could assist tumor cells in evading

Correspondence to: Zhiping Hu, Department of Abdominal Tumors II, Jiujiang Third People's Hospital, No. 408, Shili Avenue, Xunyang District, Jiujiang 332000, China
E-mail: hzp19780204@163.com

host immune surveillance within the tumor microenvironment by suppressing immune-mediated rejection response (Lin et al. 2024). At present, pembrolizumab and nivolumab, two PD-1-blocking antibodies, have been approved in combination with Ipilimumab or without for patients with metastatic CRC (Lin et al. 2023; Kciuk and Wanke 2025). Thus, investigating the regulatory mechanisms associated with PD-L1 expression in CRC is vital for gaining a deeper understanding of the function of this immunosuppressive molecule. Notably, the electron transfer flavoprotein dehydrogenase gene (ETFDH) is located in 4q32.1, which encodes the ETF-quinone oxidoreductase protein localized to the inner mitochondrial membrane (Herrero and Salegi 2024). It mediates electron transfer from flavoprotein dehydrogenase to the ubiquinone pool, playing a crucial role in the electron transport system of oxidative respiration (Liang et al. 2009). The current study has suggested that ETFDH was significantly correlated with the overall survival of CRC patients and has been identified as a potentially attractive biomarker for this tumor (Sun et al. 2020). Herein, the present work found the negative association between ETFDH and PD-L1 in CRC patients. However, whether ETFDH can regulate CRC progression through immune responses remains unknown.

Recently, the Kruppel-Like Factor (KLF) family of regulatory proteins has been identified as transcription factors that could regulate the activation and suppression of transcription by binding to DNA, RNA, and proteins, thereby affecting development, growth, metastasis, and immune response (Bushweller 2019; Yuce and Ozkan 2024). Moreover, previous studies have suggested that KLF family members are aberrantly expressed in CRC patients and partake in a variety of tumor-related biological progression (Huang and He 2022).

Table 1. Clinicopathological data of colorectal cancer patients in this study

Characteristic	Value
Total number of patients	112
Age (year)	
Median	58
Range	23–82
Sex (n)	
Male	56
Female	56
TNM stage	
I/II	40
III/IV	72
Pathologic grade	
Well	29
Moderate	62
Poor	21

Among them, KLF4 is a member of the KLF subfamily that possesses an ambivalent nature in tumorigenesis by acting as a carcinogen or tumor suppressor in a tissue-specific way (Hu et al. 2009; Qi et al. 2019). In some CRC studies, KLF4 has been reported as a tumor suppressor and hinders CRC cell proliferation and stemness by trans-activating tumor suppressor gene NDRG2 and P53 pathway-related genes (Ma et al. 2017; Yang et al. 2025). Beyond that, it has been reported that diminished expression of KLF4 could potentially activate the immune microenvironment within the CRC tumor (Yuan et al. 2024; Zhang et al. 2025). In the present work, JASPAR software initially identified that KLF4 has binding sites with the ETFDH promoter region. Moreover, ETFDH expression was negatively correlated with PD-L1 in CRC patients. Hence, this study aimed to explore whether KLF4 affects the development and immune evasion of CRC cells by targeting ETFDH.

Materials and Methods

Clinical samples and cell culture

112 CRC tumor samples and matched adjacent normal tissues were provided by the Jiujiang Third People's Hospital. Written informed consent was obtained from all subjects prior to enrollment. These excised samples were frozen and stored at −80°C. Clinicopathological data of colorectal cancer patients are shown in Table 1. The protocol of this study was authorized by the Ethics Committee of the Jiujiang Third People's Hospital and was carried out according to the guidelines of the Declaration of Helsinki.

A normal human colon mucosal epithelial cell line (NCM460) was cultured in M3 TM Base medium (M310A; INCELL Corporation, San Antonio, TX, USA). Furthermore, CRC cells (HCT 116, CL-0096; SW620, CL-0225) were maintained in media (CM-0096, CM-0225A, Procell, Wuhan, China) at 37°C with 5% CO_2.

RT-qPCR

In short, total RNAs were prepared using Trizol reagent (Invitrogen, Paisley, Scotland, UK). For cDNA synthesis, 1 μg of total RNA was reverse transcribed using HiScript 1st Strand cDNA synthesis kit (Vazyme, Nanjing, Shanghai). Reverse transcription condition: the transcription was performed in a 20 μl reaction mixture, including total RNA (100 ng), 2×Mix (10 μl), HiScript II Enzyme Mix (2 μl), Oligo $(dT)_{23}$ VN (1 μl), Random hexamers (1 μl), and RNase-free water. The total reaction mixture was incubated at 25°C for 5 min, 50°C for 15 min, and 85°C for 5 s. On the ABI 7500 fast PCR System, cDNAs were amplified using Real-time Fluorescent Quantitative PCR Kit (Vazyme). The amplification

parameters were: denaturation at 95°C for 10 min, followed by 40 cycles of denaturation at 95°C for 30 s, annealing at 60°C for 30 s and extension at 72°C for 1 min. At last, relative expression levels were standardized to that of the β-actin and analyzed utilizing $2^{-\Delta\Delta Ct}$ method. Primer sequences are presented in Table 2. This assay was conducted at least three times.

Western blot assay

In brief, clinical samples or cultured cells were washed with PBS and then lysed using RIPA lysis buffer (CST, Danvers, MA, USA). After centrifugation and mixture with loading buffer for 5–10 min at 98°C, samples were subjected to SDS-PAGE separation and electro-transfer onto PVDF membranes (Invitrogen). After blocking, the membranes were labeled with primary antibodies overnight at 4°C: ETFDH (ab103910, Abcam, Cambridge, MA, USA, 1:1000), KLF4 (ab215036, Abcam, 1:1000), PD-L1 (ab205921, Abcam, 1:1000), and β-actin (ab6276, Abcam, 1:1000). After hybridization with secondary antibodies, bands were visualized using ECL reagent. This experiment was carried out at least three times.

Cell transfection

Lentiviral pLenti-target gene construct constructs encoding human ETFDH cDNA (NM_001281738.1) or human KLF4 cDNA (NM_004235.6), and lentiviral pLKO.1 shRNA constructs targeting human ETFDH (sh-ETFDH) were provided by Addgene (Cambridge, Massachusetts, USA). In parallel, pLenti/pLKO.1 empty vector acted as a negative control (vector or sh-NC). After that, HEK293T cells at 80% confluence were individually transfected with these constructs with packaging plasmids. 72 h later, secreted virus particles in the medium were collected, and infected CRC cells with polybrene. At last, the infected cells were passaged and selected using puromycin for three days. In addition, sh-resistant ETFDH was also constructed and provided by Addgene.

EdU assay

In short, 4×10^3 CRC cells were seeded into 96-well plates and mixed with 20 μM EdU solution (Beyotime, Shanghai, China) at 37°C for 2 h. Then, the cells were washed with PBS to remove the EdU that did not penetrate into the DNA. After fixation in 4% formaldehyde, the cells were incubated in a permeabilization solution for 15 min, followed by reaction with Apollo reaction cocktail. Subsequently, the cell nuclei were stained with DAPI for 10 min and visualized using a fluorescence microscope. At last, NIS-Elements BR 3.0 software was employed to analyze the EdU-positive cells (red cells). This experiment was repeated three times.

Table 2. Primers sequences used for qPCR

Name		Primers for qPCR (5'–3')	Size (bp)
ETFDH	F:	TGCCTTGATCCAGGTGCTTT	70
	R:	GAGTGTTAAGTGGAGCCCCC	
KLF4	F:	ACCCTGGGTCTTGAGGAAGT	158
	R:	GGCATGAGCTCTTGGTAATGGA	
PD-L1	F:	ATTTGCTGAACGCCCCATAC	120
	R:	TCCAGATGACTTCGGCCTTG	
β-actin	F:	AGGATTCCTATGTGGGCGAC	273
	R:	ATAGCACAGCCTGGATAGCAA	

F, forward; R, reverse.

Colony formation assay

500 CRC cells were cultured at 37°C for approximately two weeks. Then, the visible colonies in 6-well plates were washed and fixed, followed by staining with 0.1% crystal violet. Cell colonies with >50 cells were counted and analyzed. This experiment was performed in triplicates

Transwell assay

24-well Transwell chamber with 8 μm pore inserts (Chemicon, Temecula, CA, USA) was employed to assess CRC cell migration and invasion. In short, 5×10^4 cells in 200 μl serum-free medium were added to the upper insert of Transwell chamber for migration assay, whereas 1×10^5 cells were seeded in top chamber pre-coated with 50 μl 1:8 (volume ratio) diluted Matrigel (356234, BD Biosciences, Heidelberg, Germany) for invasion assay. In parallel, the medium in the bottom counterparts harbored 10% FBS. After being incubated for 24 h, the cells on the lower surface were fixed and stained, followed by observation with an inverted microscope. This experiment was conducted at least three times.

Wound healing assay

To detect the migratory ability of CRC cells, cells were cultured in 6-well plates at 95% confluence. Then, the cell monolayer was scratched with a 200 μl sterile pipette tip (0 h). After washing, the cells were re-suspended in serum-free medium and allowed to migrate for 24 h. Representative images from the same regions of cell migration were captured by microscope at 0 h and 24 h. Finally, the distance between the two edges of the wound was analyzed using ImageJ software for the relative migration rate. This experiment was performed at least three times.

T-cell apoptosis and cytotoxicity assay

First of all, human $CD8^+$ effector T cells were isolated using EasySep™ Direct Human $CD8^+$ T cell Isolation Kit (STEMCELL, Vancouver, Canada) and activated by anti-CD3/anti-CD28, followed by re-suspending in the culture medium at 1×10^6 cells/ml. A total of 1×10^5 CRC tumor cells were counted and plated on the bottom of 24-well plates. Then, 1×10^6 activated $CD8^+$ T cells were plated in the top compartment of the Transwell at 3:1 ratio of T cells to pre-adherent CRC cells (effector-to-target). 7 h later, $CD8^+$ T cell apoptosis was stained with Annexin V-FITC and PI (Beyotime), followed by flow cytometer analysis. Meanwhile, in the co-culture system, the plates were centrifuged and the supernatant was collected. Then, the supernatant was used for the enzyme-linked immune sorbent assay (ELISA) for quantifying IFN-γ production (Beyotime). These experiments were repeated three times.

Tumor xenograft assay

In general, BALB/C male nude mice (aged 5–6 weeks, SPF Biotech, Beijing, China) were housed in specific-pathogen-free environments. Then, 5×10^6 SW620 cells or HCT 116 cells with vector or ETFDH were suspended in 100 μl PBS and subcutaneously injected into mice (n = 6 for each group). During this period, tumor volume (length×width^2/2) was determined at 5, 10, 15, 20, and 25 days after first injection. At the end of the experiment, all mice were euthanized, and the tumors were removed for imaging, weight, and Immunohistochemical (IHC) staining. This assay was authorized by the Animal Ethics Committee of the Jiujiang Third People's Hospital.

Chromatin immunoprecipitation (ChIP)

The putative KLF4 binding sites in the ETFDH promoter were assessed using SimpleChIP® Enzymatic Chromatin IP Kit (CST). To be brief, the harvested HCT 116 and SW620 cells were cross-linked with 1% formaldehyde at 37°C for 30 min, followed by termination with glycine. After being disrupted into 200–300 bp chromatin fragments using ultrasound, anti-KLF4 and anti-IgG were added. Finally, the precipitated DNA fragments were analyzed using RT-qPCR. The primers are located at −967 bp relative to transcription start site (TSS). This experiment was performed three times.

Dual-luciferase reporter assay

For ETFDH-WT/MUT reporter plasmids, the promoter regions of ETFDH with wild-type (wt) or mutant-type (mut) KLF4 binding sites were sub-cloned into the downstream of pGL3 vector (Promega, Madison, WI, USA). Then, HCT 116 and SW620 cells were transfected with recombinant vectors and sh-NC or sh-KLF4. Finally, Dual Luciferase Assay Kit (Promega) was used for the assessment of the luciferase activities. This assay was performed at least three times.

Statistical analysis

Statistical analysis and visualization were conducted based on GraphPad Prism7. Differences were deemed significant at $p < 0.05$. All results were reported as the mean ± standard deviation (SD) from at least three independent experiments. Data distribution was tested with Shapiro-Wilk test. Correlation analysis was performed using Pearson correlation analysis. Student's t-test or one-way ANOVA with Tukey's tests were employed for comparisons.

Results

Low ETFDH expression predicted a poor overall survival in CRC patients

Firstly, to identify the DEGs in CRC, the GEO2R online tool was used in three datasets, including GSE23011, GSE44076, and GSE113513. As displayed in the Venn diagram (Fig. 1A), 1 overlapping DEG (ETFDH) was identified in the three datasets. Compared to adjacent normal tissues, ETFDH expression level was significantly downregulated in CRC tumor tissues from microarray data (GSE44076 and GSE113513 databases) (Fig. 1B). To further validate the result, the GEPIA database was applied to analyze the expression of ETFDH in cancer tissues and normal samples from TCGA-COAD (T = 275 and n = 41) and TCGA-READ (T = 92 and n = 10) databases. The results exhibited that ETFDH content was obviously decreased in tumors in comparison to normal tissues (Fig. 1C). Moreover, TNMplot was utilized to evaluate the ETFDH expression profile in metastatic colorectal cancer. As shown in Figure 1D, ETFDH expression was apparently reduced in metastatic colon tissues relative to normal tissues. Consistent with the above results, RT-qPCR results verified that ETFDH was expressed at a low level in 112 CRC tumor tissues when compared to 112 adjacent normal tissues (Fig. 1E). Meanwhile, Western blot analysis exhibited a remarkable decrease in ETFDH protein levels in 6 CRC tissues (Fig. 1F). In addition, Kaplan-Meier survival analysis was performed to assess the correlation between ETFDH expression and prognosis, based on the GEPIA database. As exhibited in Figure 1G, low ETFDH expression was associated with worse overall survival. Meanwhile, based on the median value of ETFDH, 112 CRC patients were divided into the high expression group (n = 56) and the low expression group (n = 56). Then, Kaplan-Meier survival analysis also displayed that low ETFDH expression was correlated with

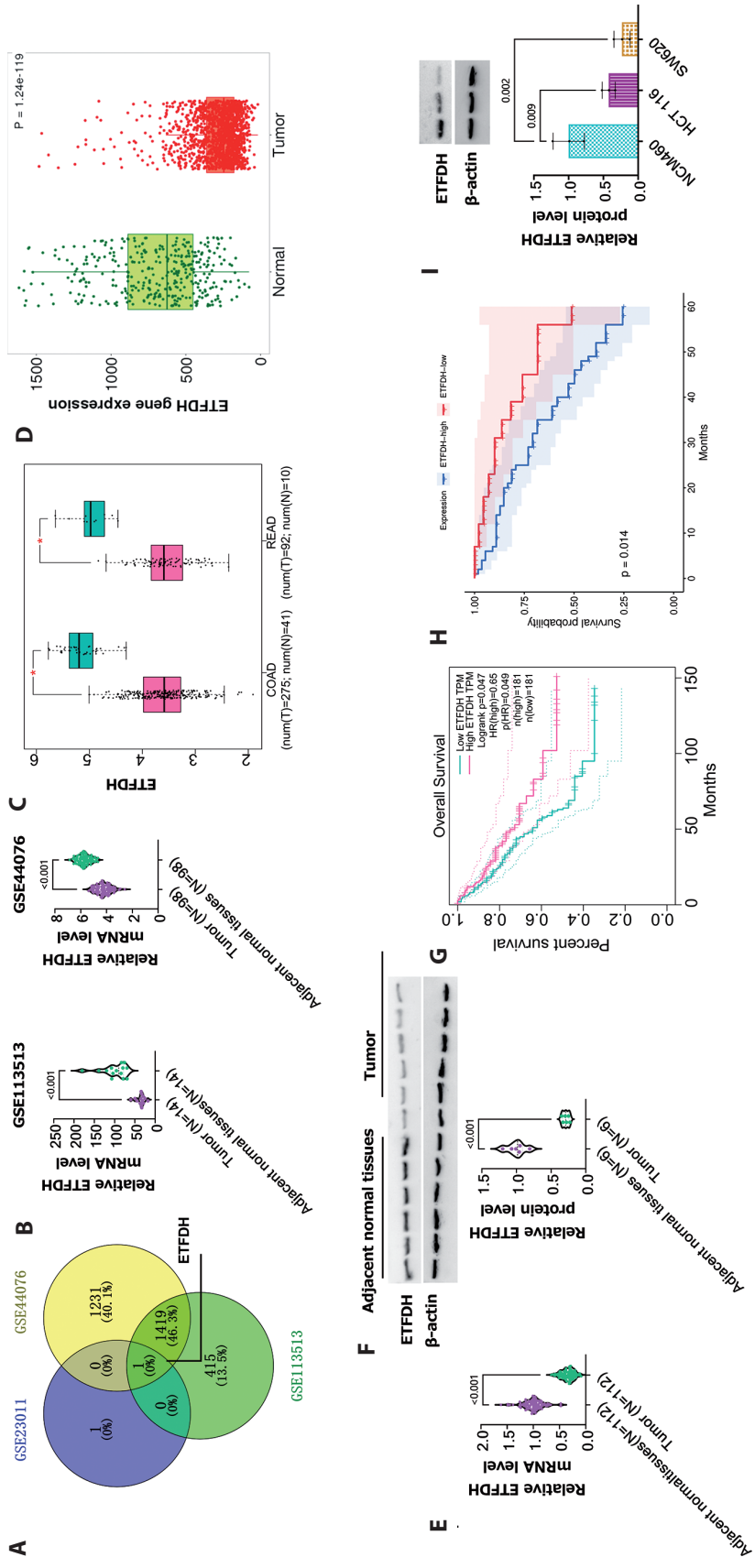

Figure 1. ETFDH was downregulated in CRC patients and cell lines. **A.** Venn diagrams showed that 1 overlap DEG was found through GEO2R in three datasets, including GSE23011, GSE44076, and GSE113513. **B.** ETFDH expression was analyzed in GSE44076 and GSE113513 databases. **C.** ETFDH expression was assessed in both TCGA-COAD (T = 275 and *N* = 41) and TCGA-READ (T = 92 and *N* = 10) databases using the GEPIA tool. **D.** Expression analysis of ETFDH in colorectal cancer by the TNMplot web tool. **E.** ETFDH mRNA level was determined in 112 pairs of CRC tumor tissues and adjacent normal tissues using RT-qPCR. **F.** ETFDH protein level was measured in 6 CRC tumor tissues and 6 adjacent normal tissues using Western blot. **G.** Kaplan-Meier plots along with GEPIA database were used to analyze the overall survival of CRC patients and ETFDH. **H.** Kaplan-Meier plot was applied to assess the overall survival of 112 clinical CRC patients. **I.** ETFDH protein level was examined in the normal human colon mucosal epithelial cell line NCM460 and CRC cells (HCT 116 and SW620) using Western blot. *n* = 3.

poorer overall survival rates (Fig. 1H). Besides, western blot results further validated that ETFDH was lower expressed in the normal human colon mucosal epithelial cell line NCM460 versus CRC cells (HCT 116 and SW620) (Fig. 1I). Together, these data suggested that ETFDH expression was decreased in CRC, and its low expression exhibited a poor prognosis in CRC patients.

Overexpressing ETFDH could block CRC cell proliferation, migration, and invasion

Subsequently, *in vitro* gain-of-function analyses were performed to determine the functional role of ETFDH in CRC cells. At first, Western blot analysis displayed that the ETFDH protein level was significantly increased in ETFDH-transfected HCT 116 and SW620 cells compared with cells with vector (Fig. 2A). After that, EdU and colony formation results showed that the numbers of EdU-positive cells and colony formation were markedly reduced by the upregulation of ETFDH in HCT 116 and SW620 cells (Fig. 2B,C). Beyond that, Transwell results showed that the upregulation of ETFDH could prominently suppress cell migration and invasion in HCT 116 and SW620 cells (Fig. 2D,E). In parallel, wound healing assay also displayed that the forced expression of ETFDH led to a significant decrease in the migration potential of HCT 116 and SW620 cells (Fig. 2F). Besides, the current data displayed that ETFDH deficiency could promote the proliferation, migration, and invasion of HCT 116 and SW620 cells, whereas these effects were partly overturned by sh-resistant ETFDH addition (Fig. S1 in Supplementary Material). Overall, these data indicated that ETFDH upregulation could inhibit CRC cell proliferation and metastasis *in vitro*.

ETFDH upregulation could suppress the apoptosis of $CD8^+$ T cells

Next, to clarify the correlation between ETFDH expression and host antitumor immune response in CRC, the expression of ETFDH and immunomodulator gene PD-L1 in CRC clini-

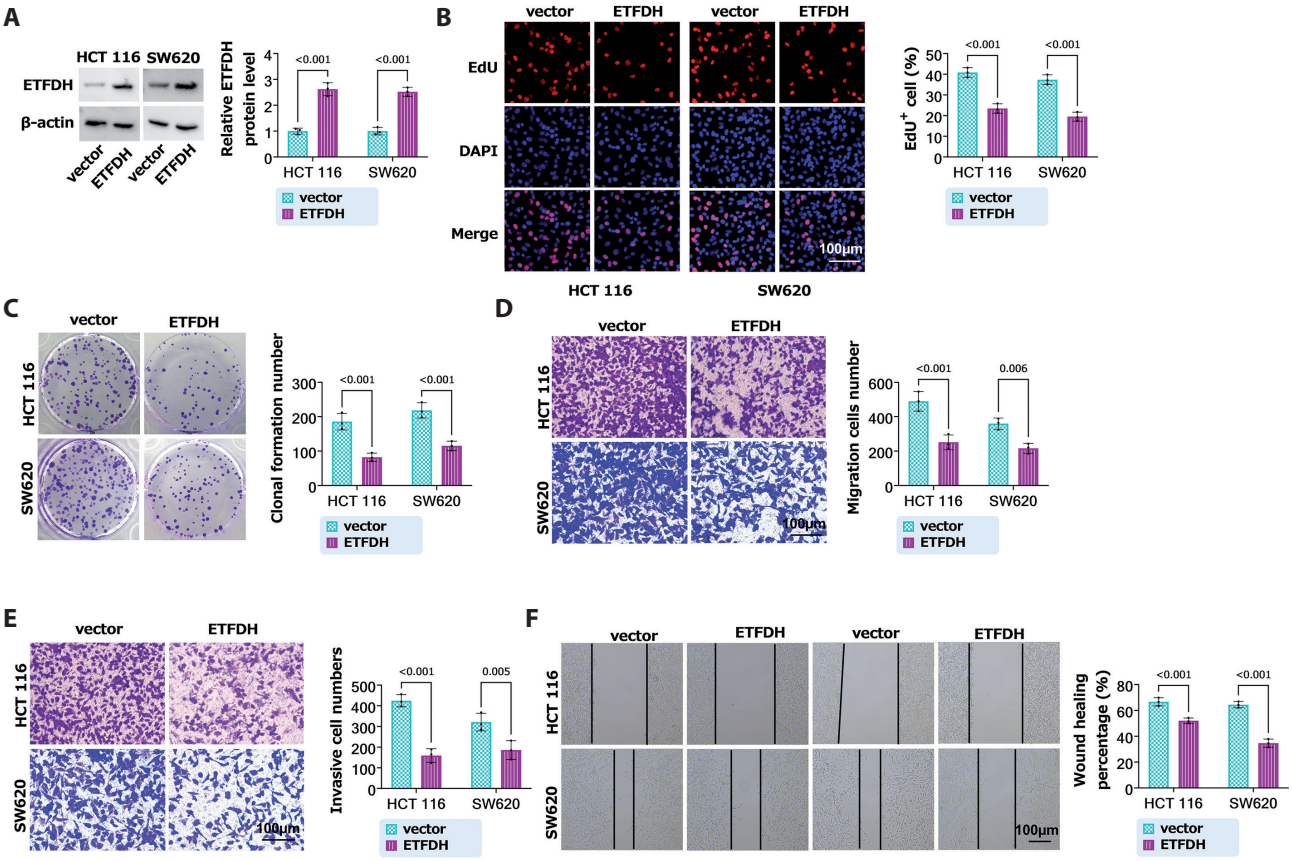

Figure 2. Effects of ETFDH on CRC cell proliferation, migration, and invasion. HCT 116 and SW620 cells were transfected with vector or ETFDH. **A.** ETFDH protein level was detected using Western blot. Cell proliferation and colony formation number were determined using EdU (**B**) and colony formation (**C**) assays. Cell migration (**D**) and invasion (**E**) were assessed using Transwell assays in transfected HCT 116 and SW620 cells. **F.** Cell migratory ability was measured using wound healing assay. $n = 3$.

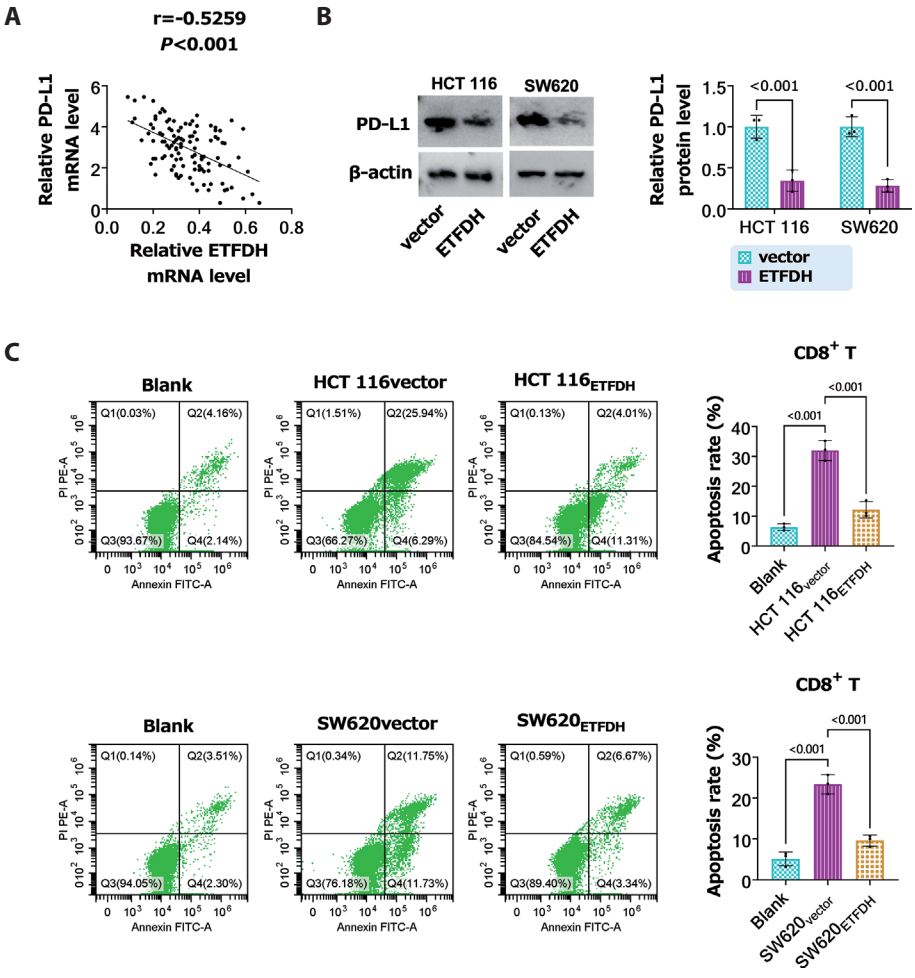

Figure 3. Effects of ETFDH upregulation on apoptosis of $CD8^+$ T cells. **A.** Pearson correlation analysis was applied to evaluate the expression association between ETFDH and immunomodulator gene PD-L1 in CRC samples. **B.** PD-L1 protein level was detected in HCT 116 and SW620 cells transfected with vector or ETFDH using Western blot assay. **C.** HCT 116 and SW620 cells were transfected with vector or ETFDH. Then, transfected HCT 116 and SW620 cells were co-cultured with isolated effector $CD8^+$ T cells, and $CD8^+$ T cell apoptosis was monitored using flow cytometry. $n = 3$.

cal samples was assessed using Pearson correlation analysis. As exhibited in Figure 3A, there was a negative correlation between ETFDH and PD-L1. Beyond that, Western blot analysis displayed that PD-L1 was obviously reduced in HCT 116 and SW620 cells after ETFDH transfection relative to the vector group (Fig. 3B). Meanwhile, RT-qPCR results showed that PD-L1 mRNA level was apparently decreased in ETFDH-transfected HCT 116 and SW620 cells (Fig. S2). After that, the influence of ETFDH overexpression on the immune response of CRC cells to T cells was further explored. On co-culturing vector or ETFDH-transfected HCT 116 and SW620 cells with $CD8^+$ T cells, flow cytometry analysis showed that the upregulation of ETFDH could effectively relieve the proportion of $CD8^+$ T cell apoptosis (Fig. 3C), while these effects were partly abolished by PD-L1 overexpression (Fig. S3), verifying that the immune effects were specifically mediated by the ETFDH/PD-L1 axis. In addition, T cells were activated with the increase in IFN-γ secretion due to ETFDH overexpression (Fig. S4), implying that tumor-infiltrating cytotoxic $CD8^+$ T cells were increased by ETFDH up-regulation. Collectively, these results suggested that ETFDH upregulation could decrease PD-L1 expression, which in turn inhibits the apoptosis of co-cultured $CD8^+$T cells *in vitro*.

Overexpressing ETFDH could block CRC cell growth in vivo

Furthermore, a xenograft mouse model of CRC was established to validate the impacts of ETFDH on tumor cell malignancy *in vivo*. Results showed smaller tumor volume and lighter tumor weight in the ETFDH group relative to the vector group (Fig. 4A,B), indicating that ETFDH upregulation could dramatically attenuate tumor growth in xenograft mouse models. Beyond that, IHC staining observed that the negative expression rate of Ki-67, MMP-9, and N-cadherin was blocked in the tissue samples from the ETFDH group compared to the vector group, whereas ETFDH expression was increased (Fig. 4C). Therefore, it is concluded that ETFDH overexpression could inhibit CRC cell growth *in vivo*.

Transcription factor KLF4 promoted the transcription of ETFDH

Then, the upstream mechanism of ETFDH was further explored in this study. Based on the JASPAR database analysis, a sequence in the ETFDH promoter was found as a putative target, and Figure 5A displayed that KLF4 binding sites in the ETFDH promoter. To validate the binding, ChIP assay was performed in HCT 116 and SW620 cells. As exhibited in Figure 5B, anti-KLF4 could elevate the enrichment of ETFDH relative to the anti-IgG group, verifying the interaction between KLF4 and ETFDH. Moreover, to further verify whether KLF4 impacts the promoter activity of ETFDH in CRC cells, a dual-luciferase reporter assay was performed. Results presented that KLF4 deficiency could obviously decrease the luciferase activity of cells expressing ETFDH-wt, rather than the mutant group (Fig. 5C), implying that KLF4 directly bound to the region of the ETFDH promoter. In addition, ETFDH mRNA level and protein level were remarkably reduced in sh-KLF4-transfected CRC cells and apparently increased in KLF4-transfected CRC cells when compared with their corresponding controls (Fig. 5D). Consistent with ETFDH expression, KLF4 content was also evidently decreased in CRC tumor tissues relative to adjacent normal tissues from microarray data (GSE44076 and GSE113513 databases) (Fig. 5E). Meanwhile, GEPIA database analysis exhibited that KLF4 expression was distinctly reduced in tumors versus normal tissues from TCGA-COAD and TCGA-READ (Fig. 5F). Consistently, RT-qPCR assay verified a significant downregulation of KLF4 in 112 CRC clinical tumor tissues compared with 112 adjacent normal tissues (Fig. 5G). Beyond that, the GEPIA database exhibited that KLF4 expression was positively associated with ETFDH in CRC tumors (Fig. 5H). Similar to the above results, Western blot assays further validated that the KLF4 protein level was strikingly decreased in CRC tumor tissues and cell lines (Fig. 5I,J). In total, these results suggested that ETFDH was the target downstream of transcription factor KLF4 in CRC cells.

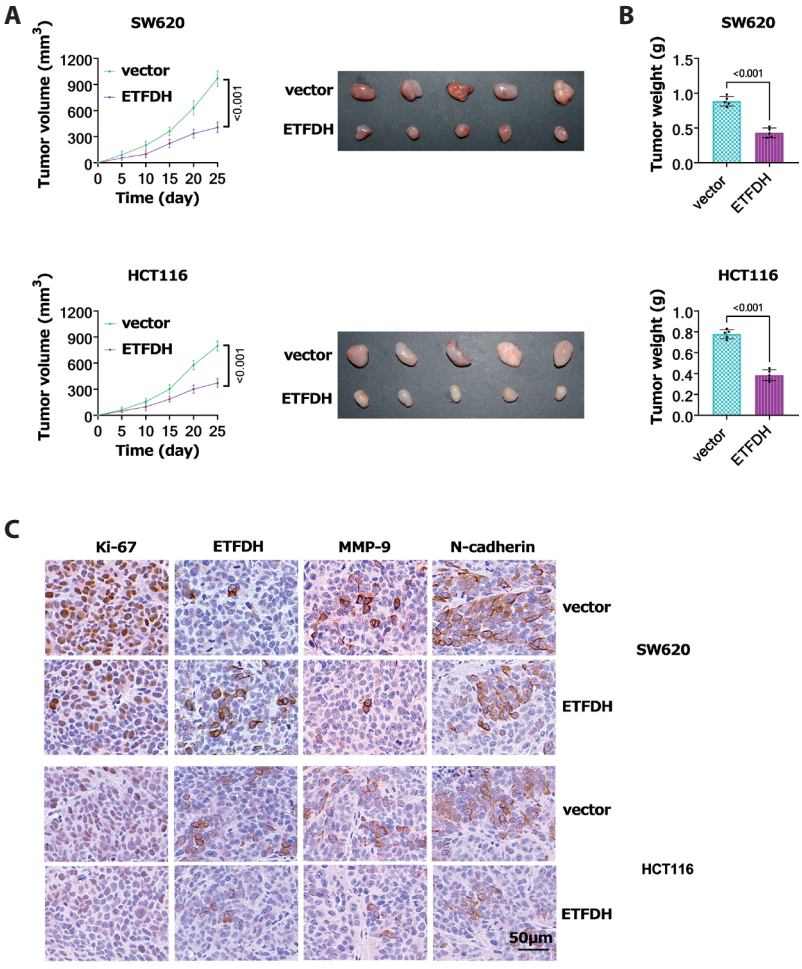

Figure 4. ETFDH upregulation suppressed CRC cell growth *in vivo*. SW620 cells and HCT 116 cells stably infected vector or ETFDH were subcutaneously inoculated into mice. **A.** Tumor growth curve of xenografts and representative image of the tumors at the end of the experiment were shown. **B.** Weight of resected tumor masses was measured. **C.** IHC staining was conducted to assess the negative expression of Ki-67, ETFDH, MMP-9, and N-cadherin in xenografts. $n = 3$.

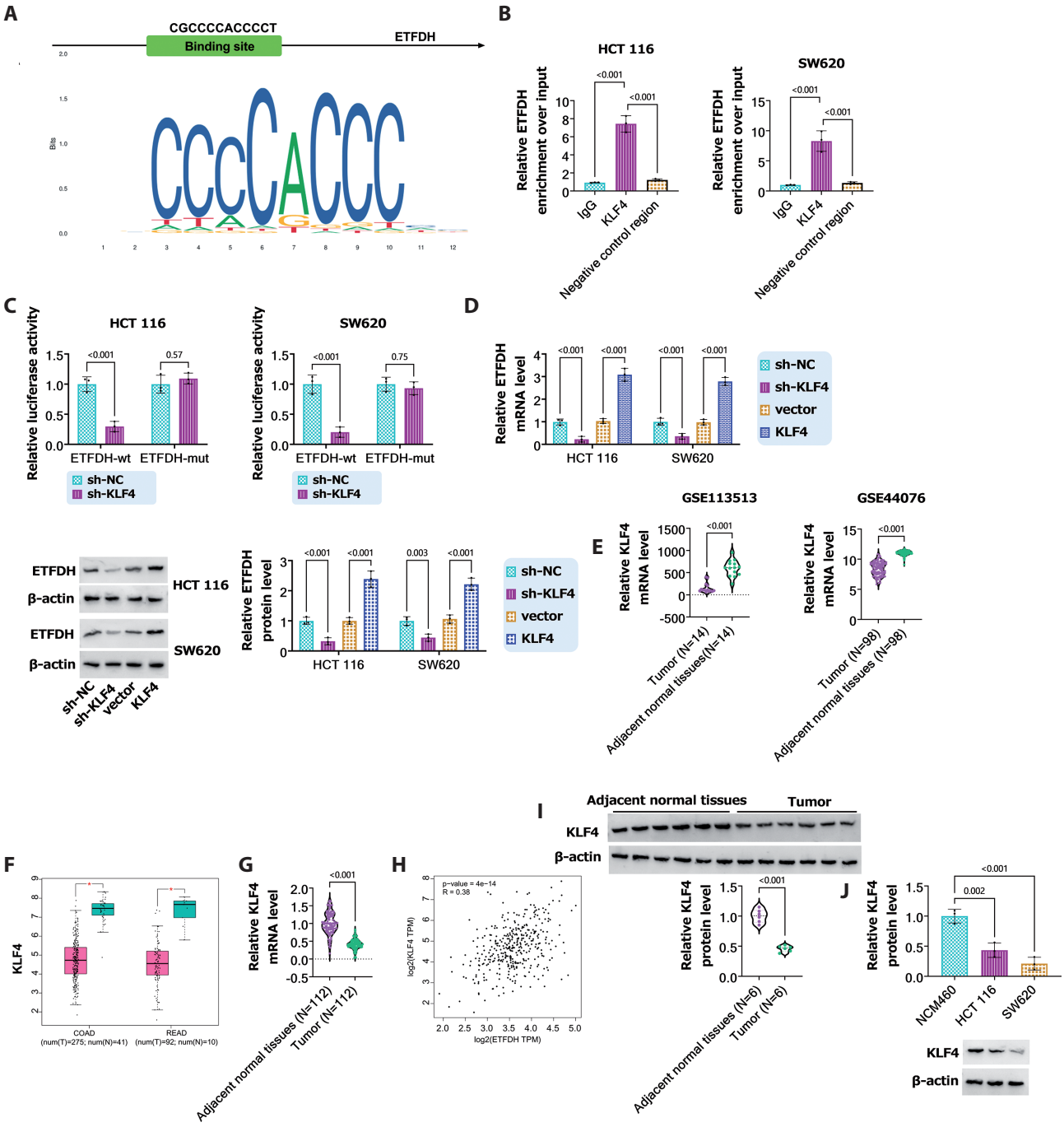

Figure 5. KLF4 activated the transcription of ETFDH. **A.** The JASPAR website was used to predict the binding of transcription factor KLF4 to the ETFDH promoter. **B.** ChIP assay was applied to assess the binding between KLF4 and ETFDH promoter. **C.** Their binding activity was analyzed using a dual-luciferase reporter assay. **D.** ETFDH mRNA level and protein level were measured in HCT 116 and SW620 cells transfected sh-NC, sh-KLF4, vector, or KLF4 using RT-qPCR and Western blot assays. **E.** Expression level of KLF4 in GSE44076 and GSE113513 databases was assessed. **F.** KLF4 level was analyzed in both TCGA-COAD (T = 275 and *N* = 41) and TCGA-READ (T = 92 and *N* = 10) databases using the GEPIA tool. **G.** RT-qPCR assay was performed to determine KLF4 mRNA level in 112 pairs of CRC tumor tissues and adjacent normal tissues. **H.** GEPIA database displayed the correlation between KLF4 and ETFDH expression in CRC tumors. **I.** Western blot analysis of KLF4 protein level in 6 CRC tumor tissues and 6 adjacent normal tissues. **J.** Western blot analysis of KLF4 protein level in normal human colon mucosal epithelial cell line NCM460 and CRC cells (HCT 116 and SW620). *n* = 3.

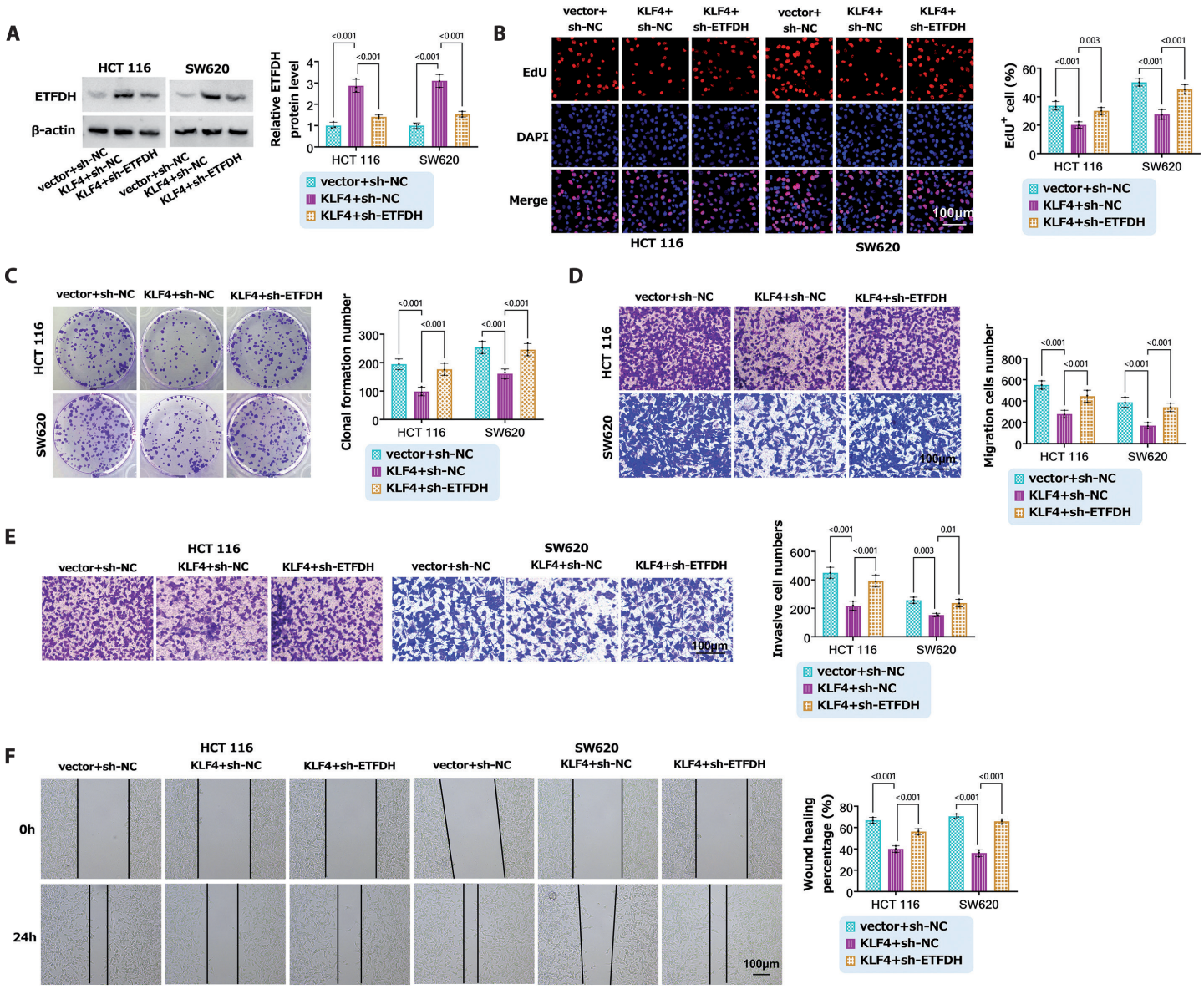

Figure 6. KLF4/ETFDH regulated CRC cell malignant behaviors. HCT 116 and SW620 cells were transfected with vector+sh-NC, KLF4+sh-NC, KLF4+sh-ETFDH. **A.** Western blot analysis of ETFDH protein level. The number of EdU-positive cells and colony formation were detected using EdU (**B**) and colony formation (**C**) assays. Transwell assays were employed to measure cell migration (**D**) and invasion (**E**) in transfected HCT 116 and SW620 cells. **F.** Wound healing assay was conducted to assess cell migratory ability. $n = 3$.

KLF4 upregulation could repress CRC cell proliferation, migration, and invasion by regulating ETFDH

Considering the modulatory role of KLF4 in ETFDH expression in CRC cells, whether the influence of KLF4 on tumor development was correlated with ETFDH was further determined. First of all, Western blot results displayed that the forced expression of KLF4 could prominently increase ETFDH protein level in HCT 116 and SW620 cells, which was partly abolished after sh-ETFDH co-transfection (Fig. 6A). Furthermore, KLF4 transfection could apparently increase KLF4 ETFDH protein level in HCT 116 and SW620 cells, whereas the knockdown of ETFDH does not affect this change (Fig. S5). Functionally, the number of EdU-positive cells and colony formation were distinctly reduced by KLF4 overexpression in HCT 116 and SW620 cells, whereas these effects were partially overturned after sh-ETFDH introduction (Fig. 6B,C). Furthermore, the inhibitory role of KLF4 upregulation on HCT 116 and SW620 cell migration and invasion was effectively ameliorated by ETFDH knockdown (Fig. 6D,E). In parallel, KLF4-mediated migratory ability suppression in HCT 116 and SW620 cells was markedly relieved through ETFDH silencing (Fig. 6F). All of these findings indicated that KLF4 overexpression could hinder CRC cell proliferation and metastasis by targeting ETFDH *in vitro*.

Elevated KLF4 could hinder the apoptosis of CD8$^+$ T cells by regulating ETFDH

Additionally, the impacts of KLF4 and ETFDH on PD-L1 expression and the apoptosis of CD8$^+$ T cells were further investigated. Subsequently, Western blot results exhibited that KLF4 upregulation could apparently dampen PD-L1 protein level in HCT 116 and SW620 cells, while these effects were partly reversed by ETFDH downregulation (Fig. 7A). After co-culturing CD8$^+$ T cells and transfected HCT

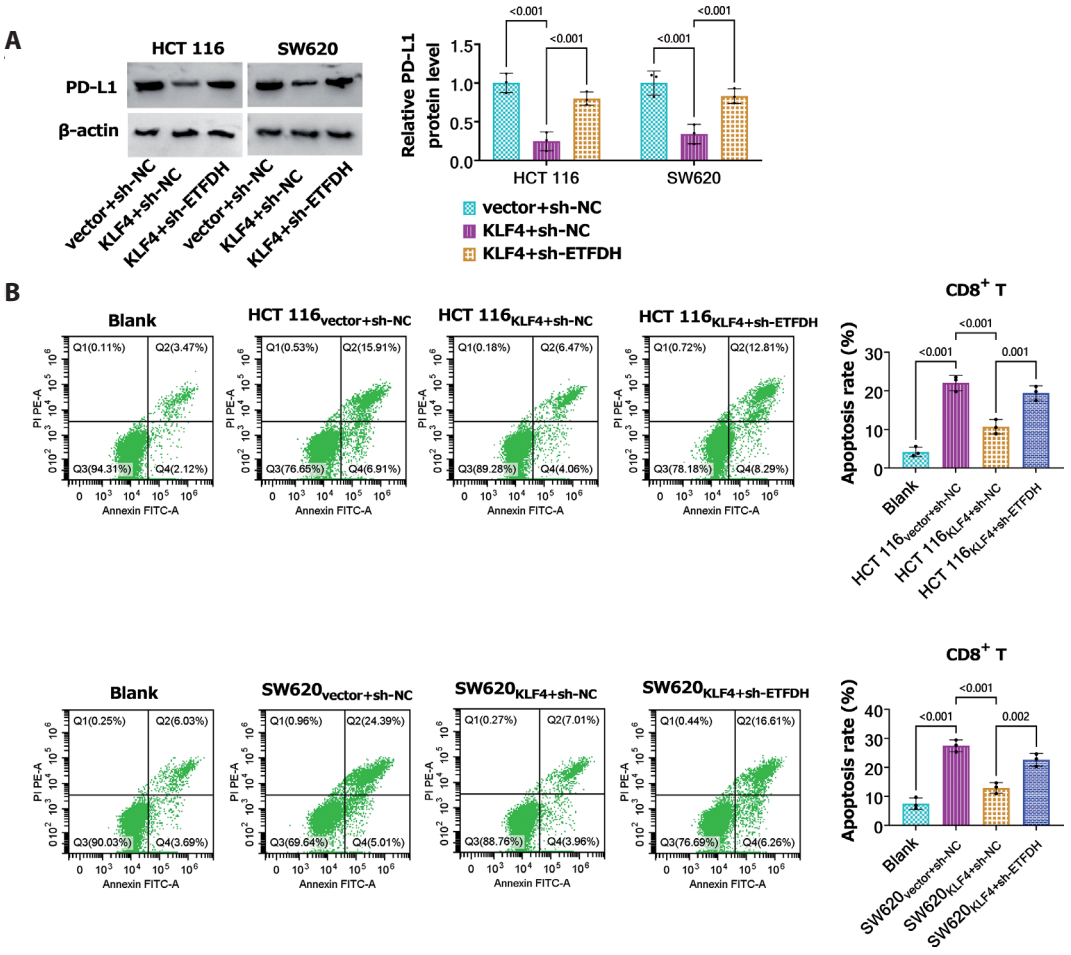

Figure 7. KLF4/ETFDH affected the apoptosis of CD8$^+$ T cells. HCT 116 and SW620 cells were transfected with vector+sh-NC, KLF4+sh-NC, KLF4+sh-ETFDH. **A.** PD-L1 protein level was examined using Western blot. **B.** The transfected HCT 116 and SW620 cells were co-cultured with isolated effector CD8$^+$ T cells. Then, flow cytometry analysis of CD8$^+$ T cell apoptosis. $n = 3$.

116 and SW620 cells, flow cytometry analysis showed that the proportion of $CD8^+$ T cell apoptosis was prominently decreased through KLF4 overexpression, which was partially attenuated after sh-ETFDH co-transfection (Fig. 7B). Collectively, these findings illuminated that KLF4 upregulation could decrease PD-L1 expression and suppress $CD8^+$ T cell apoptosis by targeting ETFDH.

Discussion

Despite encouraging advances in current immunotherapy efficacy, a substantial number of patients fail to achieve durable responses due to acquired resistance (Weng et al. 2022; Singh et al. 2024; Vahidfar et al. 2024). Notably, it has been reported that PD-L1, a primary co-inhibitory immune checkpoint protein, could form the axis with PD-1 to suppress cytotoxic T cell killing within the tumor microenvironment, thereby leading to tumor immune escape. Furthermore, conventional chemotherapeutics could also induce the expression of PD-L1 in CRC. According to these mechanistic insights, elucidating regulatory mechanisms governing PD-L1 expression in CRC has become a critical determinant for therapeutic strategy development (Yaghoubi et al. 2019; Payandeh et al. 2020). Herein, ETFDH, an inner mitochondrial membrane protein monomer, was negatively associated with PD-L1 expression in CRC patients. Furthermore, it has been reported that ETFDH is a required oxidative phosphorylation component and mediates electron transfer from flavoprotein dehydrogenases to the ubiquinone pool, resulting in ATP as the body energy supply (Herrero and Salegi 2024; Martino and D'Addabbo 2024). Interestingly, some studies have suggested that ETFDH was an independent predictor of overall survival for various human cancers (Wu et al. 2019; Wang et al. 2023), including CRC (Sun et al. 2020). Therefore, ETFDH was selected for further study.

In this study, public databases analysis found that ETFDH expression was decreased in CRC patients and related to metastatic CRC. Consistent with the former report (Sun et al. 2020), the current work verified the under-expression of ETFDH in CRC tissues and cell lines, which is significantly associated with the overall survival of CRC patients. Subsequently, functional assays exhibited that overexpressing ETFDH could hinder the proliferation, migration, and invasion of CRC cells, and block tumor growth *in vitro*. Considering the negative correlation between ETFDH and PD-L1 in CRC patients, the effects of ETFDH on $CD8^+$ T-cell-mediated immune evasion in CRC were further determined. Herein, the present research validated that ETFDH upregulation could obviously decrease PD-L1 protein level in CRC cells. Moreover, ETFDH overexpression could hinder T-cell apoptosis to reduce immune evasion by downregulating PD-L1 expression. Besides, previous studies have indicated that PD-L1 could promote tumor growth and progression by activating WIP and β-catenin signaling pathways or EGFR signaling pathway (Yu et al. 2020; Che et al. 2025). Therefore, this study inferred that ETFDH might inhibit these signaling pathways by reducing PD-L1 expression, thereby suppressing CRC tumor progression. In other words, metabolic genes can influence tumor progression through the immune-related axis. In total, these findings implied that ETFDH could inhibit CRC development and enhance CRC response to immunotherapies.

Belonging to a prominent member of the KLF subfamily of zinc finger transcription regulators, KLF4 has recently been reported as a pivotal transcriptional control and actively participates in many cellular activities, such as proliferation, invasion, cell death, differentiation, and immune regulation (Luo et al. 2022; Ju et al. 2025). Increasing evidence has discovered that KLF4 presents either tumor-suppressing or oncogenic properties in several malignant tumors (Wang et al. 2020; Ingruber and Savic 2021; He et al. 2023). It has been reported that KLF4 acts as a tumor suppressor by blocking CRC cell proliferation and immune evasion (Xiu et al. 2017; Zhang et al. 2025). Similar to transcription factors, KLF4 could exert its function via directly binding to the promoter of target genes at the transcriptional level, thereby affecting tumor progression. For example, KLF4 could transcriptionally activate NDRG2 by binding to its promoter region, thereby hindering CRC cell proliferation and tumorigenesis (Ma et al. 2017). Moreover, KLF4 could potentially regulate STAT3 expression via directly binding to its promoter, thereby activating p-STAT3 signaling and affecting CRC progression (Yuan et al. 2024). Herein, the current work displayed that KLF4 could increase ETFDH transcription by directly binding to its promoter region, validating that ETFDH is a novel KLF4-target gene. In accordance with these studies, KLF4 content was decreased in CRC patients and cells, and its overexpression could constrain CRC cell proliferation, metastasis, and repress T-cell exhaustion by regulating ETFDH. These observations further supported the KLF4/ETFDH modulatory mechanism in CRC progression. Nevertheless, there are still some shortcomings in this research. For example, the immune-related findings in this study are primarily derived from in *vitro* co-culture assays, while the in *vivo* experiments were conducted using nude mouse models, which lack mature T cells and cannot fully recapitulate intact adaptive immune responses. Consequently, although these data suggest potential immunomodulatory effects, these conclusions should be interpreted with caution. Further investigations using immunocompetent animal models are warranted to validate the proposed immune regulatory mechanisms.

Conclusion

Taken together, these findings discovered that KLF4 inhibits CRC cell growth, metastasis, and decreases $CD8^+$ T cell

exhaustion-like phenotype through mediating transcriptional upregulation of ETFDH, which provides a potential therapeutic target for CRC.

Ethics approval and consent to participate. The protocols of this study were authorized by the Ethics Committee of the Jiujiang Third People's Hospital and were carried out according to the guidelines of Declaration of Helsinki. Written informed consent was obtained from all subjects prior to enrollment. This assay was authorized by the Animal Ethics Committee of the Jiujiang Third People's Hospital.

Data availability statement. The datasets are available from the corresponding author on reasonable request.

Conflict of interest. The authors declare that they have no conflict of interest.

Author contributions. YZ conducted the experiments and drafted the manuscript. QL collected and contributed the methodology. YX analyzed the data, operated the software and edited the manuscript. TZ prepared figures. ZH designed and supervised the study. All authors read and approved the final manuscript.

References

Abedizadeh R, Majidi F, Khorasani HR, Abedi H, Sabour D (2024): Colorectal cancer: a comprehensive review of carcinogenesis, diagnosis, and novel strategies for classified treatments. Cancer Metastasis Rev **43,** 729-753 https://doi.org/10.1007/s10555-023-10158-3

Biller LH, Schrag D (2021): Diagnosis and treatment of metastatic colorectal cancer: A Review. JAMA **325,** 669-685 https://doi.org/10.1001/jama.2021.0106

Bushweller JH (2019): Targeting transcription factors in cancer - from undruggable to reality. Nat Rev Cancer **19,** 611-624 https://doi.org/10.1038/s41568-019-0196-7

Che S, Zhang Y, Xu H, Shi J, Hou Y (2025): TBB inhibits CK2/PD-L1/EGFR pathway-mediated tumor progression. Eur J Pharmacol **999,** 177689 https://doi.org/10.1016/j.ejphar.2025.177689

Ganesh K, Stadler ZK, Cercek A, Mendelsohn RB, Shia J (2019): Immunotherapy in colorectal cancer: rationale, challenges and potential. Nat Rev Gastroenterol Hepatol **16,** 361-375 https://doi.org/10.1038/s41575-019-0126-x

He Z, He J, Xie K (2023): KLF4 transcription factor in tumorigenesis. Cell Death Discov **9,** 118 https://doi.org/10.1038/s41420-023-01416-y

Herrero Martín JC, Salegi Ansa B (2024): An ETFDH-driven metabolon supports OXPHOS efficiency in skeletal muscle by regulating coenzyme Q homeostasis. Nat Metab **6,** 209-225 https://doi.org/10.1038/s42255-023-00956-y

Hu W, Hofstetter WL, Li H, Zhou Y, He Y, Pataer A, Wang L, Xie K, Swisher SG, Fang B (2009): Putative tumor-suppressive function of Kruppel-like factor 4 in primary lung carcinoma. Clin Cancer Res **15,** 5688-5695 https://doi.org/10.1158/1078-0432.CCR-09-0310

Huang Z, He H (2022): Expression and Prognosis value of the KLF family members in colorectal cancer. J Oncol **2022,** 6571272 https://doi.org/10.1155/2022/6571272

Ingruber J, Savic D (2021): KLF4, Slug and EMT in head and neck squamous cell carcinoma. Cell **10,** 539 https://doi.org/10.3390/cells10030539

Ju Y, Xiao W, Mathis BJ, Shi Y (2025): KLF4: a multifunctional nexus connecting tumor progression and immune regulation. Front Immunol **16,** 1514780 https://doi.org/10.3389/fimmu.2025.1514780

Kciuk M, Wanke K (2025): Focus on PD-1/PD-L1-targeting antibodies in colorectal cancer: Are there options beyond dostarlimab, nivolumab, and pembrolizumab? A Comprehensive Review. Molecules **30,** 2686 https://doi.org/10.3390/molecules30132686

Lee D, Cho M, Kim E, Seo Y, Cha JH (2024): PD-L1: From cancer immunotherapy to therapeutic implications in multiple disorders. Mol Ther **32,** 4235-4255 https://doi.org/10.1016/j.ymthe.2024.09.026

Liang WC, Ohkuma A, Hayashi YK, López LC, Hirano M, Nonaka I, Noguchi S, Chen LH, Jong YJ, Nishino I (2009): ETFDH mutations, CoQ10 levels, and respiratory chain activities in patients with riboflavin-responsive multiple acyl-CoA dehydrogenase deficiency. Neuromuscul Disord **19,** 212-216 https://doi.org/10.1016/j.nmd.2009.01.008

Lin KX, Istl AC, Quan D, Skaro A, Tang E, Zheng X (2023): PD-1 and PD-L1 inhibitors in cold colorectal cancer: challenges and strategies. Cancer Immunol Immunother **72,** 3875-3893 https://doi.org/10.1007/s00262-023-03520-5

Lin X, Kang K, Chen P, Zeng Z, Li G, Xiong W, Yi M, Xiang B (2024): Regulatory mechanisms of PD-1/PD-L1 in cancers. Mol Cancer **23,** 108 https://doi.org/10.1186/s12943-024-02023-w

Luo X, Zhang Y, Meng Y, Ji M, Wang Y (2022): Prognostic significance of KLF4 in solid tumours: an updated meta-analysis. BMC Cancer **22,** 181 https://doi.org/10.1186/s12885-022-09198-9

Ma Y, Wu L, Liu X, Xu Y, Shi W, Liang Y, Yao L, Zheng J, Zhang J (2017): KLF4 inhibits colorectal cancer cell proliferation dependent on NDRG2 signaling. Oncol Rep **38,** 975-984 https://doi.org/10.3892/or.2017.5736

Martino S, D'Addabbo P (2024): Deep intronic ETFDH variants represent a recurrent pathogenic event in multiple acyl-CoA dehydrogenase deficiency. Int J Mol Sci **25,** 9637 https://doi.org/10.3390/ijms25179637

Mou F, Sun Q, Ye Z (2025): Advances in the combination of immunotherapy and radiotherapy for microsatellite-stable metastatic colorectal cancer. Curr Proteomics **22,** 100049 https://doi.org/10.1016/j.curpro.2025.100049

Qi XT, Li YL, Zhang YQ, Xu T, Lu B, Fang L, Gao JQ, Yu LS, Zhu DF, Yang B (2019): KLF4 functions as an oncogene in promoting cancer stem cell-like characteristics in osteosarcoma cells. Acta Pharmacol Sin **40,** 546-555 https://doi.org/10.1038/s41401-018-0050-6

Qu R, Ma Y, Zhang Z, Fu W (2022): Increasing burden of colorectal cancer in China. Lancet Gastroenterol Hepatol **7,** 700 https://doi.org/10.1016/S2468-1253(22)00156-X

Shin AE, Giancotti FG, Rustgi AK (2023): Metastatic colorectal cancer: mechanisms and emerging therapeutics. Trends Pharmacol Sci **44,** 222-236
https://doi.org/10.1016/j.tips.2023.01.003

Singh M, Morris VK, Bandey IN, Hong DS, Kopetz S (2024): Advancements in combining targeted therapy and immunotherapy for colorectal cancer. Trends Cancer **10,** 598-609
https://doi.org/10.1016/j.trecan.2024.05.001

Sun Z, Liu C, Cheng SY (2020): Identification of four novel prognosis biomarkers and potential therapeutic drugs for human colorectal cancer by bioinformatics analysis. J Biomed Res **35,** 21-35
https://doi.org/10.7555/JBR.34.20200021

Vahidfar N, Ahmadzadehfar H, Farzanefar S, Abbasi M, Salehi Y, Saboktakin F, Jahanbin M, Kashi MB, Eppard E, Biersack HJ (2024): Optimal indications of radioimmunotherapy in nuclear medicine: A Mini-Review. Curr Radiopharm **17,** 320-329
https://doi.org/10.2174/0118744710295825240308093429

Wang X, Xia S, Li H, Wang X (2020): The deubiquitinase USP10 regulates KLF4 stability and suppresses lung tumorigenesis. Cell Death Differ **27,** 1747-1764
https://doi.org/10.1038/s41418-019-0458-7

Wang X, Zhou L, Dong Z, Wang G (2023): Identification of iron metabolism-related predictive markers of endometriosis and endometriosis-relevant ovarian cancer. Medicine **102,** e33478
https://doi.org/10.1097/MD.0000000000033478

Weng J, Li S, Zhu Z, Liu Q, Zhang R, Yang Y, Li X (2022): Exploring immunotherapy in colorectal cancer. J Hematol Oncol **15,** 95
https://doi.org/10.1186/s13045-022-01294-4

Wu Y, Zhang X, Shen R, Huang J, Lu X, Zheng G, Chen X (2019): Expression and significance of ETFDH in hepatocellular carcinoma. Pathol Res Pract **215,** 152702
https://doi.org/10.1016/j.prp.2019.152702

Xiu DH, Chen Y, Liu L, Yang HS, Liu GF (2017): Tumor-suppressive role of Kruppel-like factor 4 (KLF-4) in colorectal cancer. Genet Mol Res **16,** 9272
https://doi.org/10.4238/gmr16019272

Yaghoubi N, Soltani A, Ghazvini K, Hassanian SM, Hashemy SI (2019): PD-1/ PD-L1 blockade as a novel treatment for colorectal cancer. Biomed Pharmacother **110,** 312-318
https://doi.org/10.1016/j.biopha.2018.11.105

Yang HJ, Kim EJ, Kim Y (2025): ACTL6A depletion induces KLF4-mediated anti-tumorigenic effects in colorectal cancer. Cell Death Dis **16,** 653
https://doi.org/10.1038/s41419-025-07946-w

Yu W, Hua Y, Qiu H, Hao J, Zou K, Li Z, Hu S, Guo P, Chen M, Sui S (2020): PD-L1 promotes tumor growth and progression by activating WIP and β-catenin signaling pathways and predicts poor prognosis in lung cancer. Cell Death Dis **11,** 506
https://doi.org/10.1038/s41419-020-2701-z

Yuan L, Meng Y, Xiang J (2024): KLF4 induces colorectal cancer by promoting EMT via STAT3 activation. Dig Dis Sci **69,** 2841-2855
https://doi.org/10.1007/s10620-024-08473-y

Yuce K, Ozkan AI (2024): The kruppel-like factor (KLF) family, diseases, and physiological events. Gene **895,** 148027
https://doi.org/10.1016/j.gene.2023.148027

Zhang C, Yi S, Cao X, Wang J (2025): Modulating colorectal cancer cell propagation and immune evasion by miRNA-148a-3p via KLF4. Iran J Allergy Asthma Immunol **24,** 481-497

Received: February 5, 2026
Final version accepted: May 29, 2026